Acta Biochim Biophys Sin 2022, 54(11): 1731–1739
https://doi.org/10.3724/abbs.2022173
Advance Access Publication Date: 24 November 2022
Original Article

Original Article

KRAS G12D mutation eliminates reactive oxygen species through the Nrf2/CSE/H_2S axis and contributes to pancreatic cancer growth

Kun Fan[1,2,3,4,5,†], Shulong Zhang[1,†], Xiaojian Ni[2,3,4,5], Sheng Shen[1,2,3,4,5], Jiwen Wang[2,3,4,5], Wentao Sun[2,3,4,5], Tao Suo[2,3,4,5], Han Liu[2,3,4,5], Xiaoling Ni[2,3,4,5,*], and Houbao Liu[1,2,3,4,5,*]

[1]Department of General Surgery, Central Hospital of Xuhui District,Shanghai 200032, China, [2]Department of General Surgery, Zhongshan Hospital, Fudan University, Shanghai 200032, China, [3]Biliary Tract Disease Center of Zhongshan Hospital, Fudan University, Shanghai 200032, China, [4]Biliary Tract Disease Institute, Fudan University, Shanghai 200032, China, and [5]Cancer Center, Zhongshan Hospital, Fudan University, Shanghai 200032, China

[†]These authors contributed equally to this work.

*Correspondence address. Tel: +86-21-31017420; E-mail: liu.houbao@zs-hospital.sh.cn (H.L.) / E-mail: ni.xiaoling@zs-hospital.sh.cn (X.N.)

Received 27 July 2021 Accepted 9 February 2022

Abstract

In pancreatic cancer, KRAS G12D can trigger pancreatic cancer initiation and development. Rapid tumor growth is often accompanied by excess intracellular reactive oxygen species (ROS) production, which is unfavorable to tumor. However, the regulation of intracellular ROS levels in KRAS mutant pancreatic cancer remains unclear. In this study, we establish BxPC3 stable cell strains expressing KRAS wild type (WT) and G12D mutation and find unchanged ROS levels despite higher glycolysis and proliferation viability in KRAS mutant cells than KRAS WT cells. The key hydrogen sulfide (H_2S)-generating enzyme cystathionine-γ-lyase (CSE) is upregulated in KRAS mutant BxPC3 cells, and its knockdown significantly increases intracellular ROS levels and decreases cell glycolysis and proliferation. Nuclear factor erythroid 2-related factor 2 (Nrf2) is activated by KRAS mutation to promote CSE transcription. An Nrf2 binding site (–47/–39 bp) in the CSE promoter is verified. CSE overexpression and the addition of NaHS after Nrf2 knockdown or inhibition by brusatol decreases ROS levels and rescues cell proliferation. Our study reveals the regulatory mechanism of intracellular ROS levels in KRAS mutant pancreatic cancer cells, which provides a potential target for pancreatic cancer therapy.

Key words KRAS mutation, Nrf2, CSE, ROS, pancreatic cancer

Introduction

Pancreatic ductal adenocarcinoma (PDAC) is a highly malignant cancer with poor prognosis, and the five-year survival rate remains only 9% [1,2]. The whole-genome sequence redefines the mutational landscape of pancreatic cancer, which makes potential preparations for targeted therapy [3]. KRAS activating mutations occur in 70%–95% of pancreatic cancer cases [3,4]. Moreover, the oncogene *KRAS* is frequently mutationally activated in many kinds of tumors, affecting a multitude of cellular processes [5–7]. Therefore, targeting KRAS mutations is prospectively considered for pancreatic cancer therapy [7]. A majority of KRAS mutations (95%) occur at G12 (more than 80%) and G13, including G12D, G12V, G12C, G12A, G12S and G12R mutations, and G12D is the most predominant mutation [7,8]; and KRAS mutations at G13 are rare [9]. KRAS mutations at G12 represent different roles in tumors, and there are no effective therapies targeting KRAS mutations in pancreatic cancer [7]. KRAS G12R mutation fails to bind with the PI3K catalytic subunit p110α, resulting in a distinct drug sensitivity profile compared with KRAS G12D mutation [7]. An inhibitor targeting KRAS G12C mutation is an emerging premise, entering clinical evaluation [7], but prior efforts are hampered by adaptive feedback reactivation of wild-type RAS [10]. KRAS G12D mutation accounts for 50% of all mutations, suggesting its important roles in pancreatic cancer [11,12]. Several studies have confirmed the roles of KRAS G12D mutation in PDAC initiation and progression [12–16]. Our previous study indicated that KRAS G12D mutation

enriches Treg to cause immune escape of pancreatic cancer [4]. More attention is given to KRAS G12D mutation in pancreatic cancer.

Reactive oxygen species (ROS) are mainly generated from metabolic reactions in mitochondria [17,18]. To some extent, ROS promote tumor progression. However, the accumulation of ROS can damage DNA, RNA, lipid, protein and other intracellular molecules [17,19]. Therefore, multiple antioxidative defense mechanisms are generated in tumors [17]. It remains unclear how impairments of excessive ROS are alleviated in pancreatic cancer. cystathionine-γ-lyase (CSE) is a key enzyme that converts cystathionine to L-cysteine and generates endogenous H_2S [20,21]. As a reductant, H_2S can regulate cellular redox equilibrium [22]. Moreover, H_2S is the third gas transmitter and plays important roles in multiple physiological processes, including vasorelaxation, angiogenesis, cellular energy production, neuromodulation, cytoprotection and pathological processes, including cardiac fibrosis, inflammation, obesity, diabetes, atherosclerosis and hypertension [21]. Upregulation of H_2S-producing enzyme expression has also been confirmed in various kinds of cancers [23]. Exogenous administration of NaHS promotes the proliferation of human colon cancer HCT116 cells [24]. Our previous study also suggested the important roles of CSE/H_2S in promoting colon cancer [21]. However, the roles of CSE and H_2S products in pancreatic cancer remain unclear.

In this study, we revealed that KRAS G12D mutation promoted CSE transcription through Nrf2, in which the H_2S product eliminated excess ROS and promoted pancreatic cancer cell proliferation. The modulation of ROS levels provides a potential target for KRAS mutant pancreatic cancer therapy.

Materials and Methods

Cell culture and transfection

Human pancreatic cancer cell lines BxPC3 and SW1990 (with KRAS G12D mutation) were purchased from the Type Culture Collection of the Chinese Academy of Sciences (Shanghai, China) and cultured in DMEM (G4510; Servicebio, Wuhan, China) supplemented with 10% fetal bovine serum, 100 U/mL penicillin, and 100 μg/mL streptomycin in a 37°C incubator with 5% CO_2 supply. RNA interference (RNAi) experiments were performed using commercially synthetic siRNA oligonucleotides (GenePharma, Shanghai, China). The siRNAs of CSE and Nrf2 were following: si-CSE1, 5′-GCGUUGGUAUUUCACAUUCAA-3′; si-CSE2, 5′-CGCAUCAUUAUUGAAGAACUA-3′; si-Nrf2-1, 5′-GCUCCUACUGUGAUGUGAAAU-3′; si-Nrf2-2, 5′-CCGGCAUUUCACUAAACACAA-3′; si-NC, 5′-UUCUCCGAACGUGUCACGUTT-3′. Cells were seeded to 6-well dishes and transfected at 60% density for 48 h via Lipofectamine™ 2000 transfection reagent (Thermofisher) according to the manufacturer's instructions. Before siRNA transfection, medium was replaced by serum-free DMEM. Then 5 μL siRNA (20 μM) was mixed with 250 μL serum-free DMEM for 5 min, and 5 μL lipo2000 was mixed with 250 μL serum-free DMEM for 5 min. The siRNA solution was mixed with Lipofectamine™ 2000 transfection reagent for 20 min, then added to cells. Cell medium was changed to high glucose DMEM with 10% serum after 6 h. Knockdown efficiency was detected through western blot analysis.

Stable cell establishment

The stable cells with CSE knockdown and KRAS overexpression were established respectively. shNC sequence was 5′-CCGGTTTCTCCGAACGTGTCACGTTTCAAGAGAACGTGACACGTTCGGAGAATTTTTG-3′, shCSE sequence was 5′-CCGGTGCGTTGGTATTTCACATTCAATTCAAGAGATTGAATGTGAAATACCAACGCTTTTTG-3′. These sequences were synthesized (GENEWIZ, Suzhou, China) and cloned into a pLKO.1 vector. Approximately 10 μg shCSE or shNC plasmid was co-transfected with 6 μg pCMV-ΔR8.2 and 4 μg pCMV-VSVG plasmids to 293T cells for 48 h at 50% confluence. The cell supernatant was collected and filtered with a 0.45 μm filter to transfect SW1990 cells. After screening via 2 μg/μL puromycin for one week, the stable cells with CSE knockdown were detected through western blot analysis. KRAS sequence (NM_033360.4) was synthesized (GENEWIZ, Suzhou, China) and cloned into a pQCIH vector. G12D mutation was performed through replacing adenine with guanine at 35. Similarly, approximately 10 μg WT or G12D KRAS plasmid (GENEWIZ) was co-transfected with 6 μg pCMV-ΔR8.2 and 4 μg pCMV-VSVG plasmids to 293T cells for 48 h at 50% confluence. Then cell supernatant was collected and filtered to transfect BxPC3 cells. BxPC3 stable cells with KRAS overexpression were screened by 2 μg/μL puromycin for one week and detected through western blot analysis.

Antibodies and reagents

Anti-RAS antibody (GB11411), anti-histone H3 antibody (GB13102) and anti-actin antibody (GB12001) were purchased from Servicebio. Anti-phospho-p44/42 MAPK (ERK1/2) antibody (4377) and anti-p44/42 MAPK antibody (4695) were purchased from Cell Signaling Technology (Danvers, USA). Nrf2 antibody (ab62352), CBS antibody (ab140600) and CTH antibody (ab189916) were purchased from Abcam (Cambridge, USA). Flag-tagged antibody (AE063) and HA-tagged antibody (AE036) were purchased from Abclonal (Wuhan, China). Brusatol (S7956) was purchased from Selleck (Shanghai, China).

Real-time PCR

Cells were first lysed by TRIzol (ThermoFisher) for RNA extraction as previously described [25]. The total RNA concentration was measured, and 2 μg of total RNA was reverse transcribed to cDNA using the PrimeScript™ RT Master Mix kit (RR036A; TaKaRa, Dalian, China) according to the manufacturer's guidelines. The cNDA concentration was adjusted to 100 ng/μL for real-time PCR. The 10 μL reaction volume included 5 μL TB Green Premix, 4.5 μL cDNA, 0.2 μL forward primer, 0.2 μL reverse primer and 0.1 μL ROX II. Finally, real-time PCR was performed using an Applied Biosystems 7500 Fast real-time PCR System (Applied Biosystems, Foster City, USA). Real-time PCR primers are as follows: *actin* forward primer, 5′-ACAGAGCCTCGCCTTTGC-3′, reverse primer, 5′-CCACCATCACGCCCTGG-3′; *CSE* forward primer, 5′-AGCCTTCATAATAGACTTCG-3′, reverse primer, 5′-CAGCCCAGGATAAATAAC-3′; and *CBS* forward primer, 5′-GCGGCTGAAGAACGAAATCC-3′, reverse primer, 5′-TGTCCAGCTTCCCATCACAC-3′. The gene expression levels were calculated using the $2^{-\Delta\Delta Ct}$ method, and *actin* was used as the internal control.

Nuclear and cytoplasmic protein extraction

Nuclear and cytoplasmic proteins were isolated using the Nuclear and Cytoplasmic Protein Extraction Kit (C510001; Sangon Biotech, Shanghai, China) according to the manufacturer's instructions. Briefly, cells were scraped off with cold PBS and then centrifuged at 1000 *g* at 4°C for 3 min. The supernatant was removed, and cell

debris was mixed with 200 μL buffer A (10 mM HEPES, pH 7.5, 10 mM KCl, 1.5 mM $MgCl_2$, 1 mM glycerol phosphate, 0.5 mM DTT, 1 mM NaF) and lysed for 15 min on ice. Then, 11 μL buffer B (buffer A + 0.15% Nonidet P-40) was added, mixed, and centrifuged at 14,000 *g* for 5 min. The cytoplasmic protein within the upper supernatant was harvested. The white nuclear deposit was mixed with 100 μL buffer C (20 mM HEPES, pH 7.5, 420 mM NaCl, 1.5 mM $MgCl_2$, 0.5 mM DTT, 1 mM NaF, 1 mM glycerol phosphate), lysed for 40 min on ice, and then centrifuged at 14,000 *g* for 5 min. The nuclear and cytoplasmic proteins were detected by western blot analysis.

ECAR (extracellular acidification rate) assay

The ECAR assay was performed with a Seahorse XF24 instrument (Agilent, Palo Alto, USA) within two days. Cells were seeded into Seahorse XF24 tissue culture plates, and sensor hydration was performed on the first day. BxPC3 cells or SW1990 cells were dissociated with trypsin and resuspended in base medium at a concentration of 2×10^5 cells/mL. Approximately 100 μL of cell suspension was plated into each well of the plate and incubated for 4 h. Then, 150 μL of growth medium was added to each well for cell growth overnight in a cell incubator. Meanwhile, the sensor cartridge (sensors up) was placed next to the calibration plate, and then 1 mL of Seahorse XF Calibrant was added to each well in a 37°C incubator without CO_2 overnight. The XF24 analyzer was also run overnight with XF24 software. The assay media and compounds were prewarmed, the media in the Seahorse XF24 tissue culture plate was exchanged, and the final volume remained at 575 μL. Approximately 100 μL of compounds was loaded into the appropriate port of the cartridge, which was placed back into the incubator without CO_2 to heat up to 37°C. Finally, the assay template was loaded for the ECAR assay.

Cell viability and colony formation assay

Cell viability was detected as described previously [26]. Cells were seeded into 96-well plates at 5000 cells per well. After 12 h, 10 μL CCK8 reagent (CK04; Dojindo Laboratories, Kumamoto, Japan) was added to each well and incubated for 30 min at 37°C. Then the optical density of each well was detected by the Infinite® 200 PRO microplate reader (Tecan, Männedorf, Switzerland) at 450 nm, and the time was marked as the beginning time. Cell viability was assayed every 24 h. Then, clone formation assay was performed as described previously [26]. Briefly, cells were digested and adjusted to a density of 1×10^4 cells/mL, and approximately 1000 cells were seeded into each well of 6-well plates and cultured for approximately ten days. Finally, the cells were stained with crystal violet (G1014; Servicebio), and the number of colonies (a dot with more than 100 cells) was counted.

ROS assay

Intracellular ROS levels were detected using an ROS Assay Kit (50101ES01; Yeasen, Shanghai, China). First, the DCFH-DA fluorescent dyes were diluted in serum-free DMEM at 1:1000. The treated cells were incubated with DCFH-DA solution at 37°C for 30 min and washed with PBS twice. Finally, intracellular ROS levels were detected by a BD Fortessa flow cytometer (BD Biosciences).

Apoptosis assay

Cell apoptosis was detected using an apoptosis assay kit (556547; BD Biosciences, Franklin Lakes, USA). Cells were seeded into 6-well plates for treatment. After that, the cells were washed twice with PBS and resuspended in 1 × binding buffer. Then, 5 μL of FITC Annexin V and 5 μL PI were added and incubated for 15 min at room temperature in the dark. Finally, 400 μL of 1 × binding buffer was added to each tube, and the cell samples were analyzed by the BD Fortessa flow cytometer.

Xenograft tumor assay

The nude mouse xenograft tumor model was established in accordance with the approved guidelines of the Animal Ethical Committee of Zhongshan Hospital affiliated with Fudan University. SW1990 cells were employed to establish stable cells with CSE knockdown through shCSE1, and shNC was used as a control. BALB/c nude mice (4- to 5-week-old, male) were subcutaneously injected with approximately 2×10^6 SW1990 cells. The xenograft tumor was monitored every other day and grown for approximately 35 days for analysis.

Dual luciferase reporter assay

SV40 plasmids express Renilla luciferase, and pGL3-basic plasmids express firefly luciferase. The DNA fragment (–900/ + 50 bp) of the *CSE* promoter was synthesized and cloned into pGL3-basic vectors to construct luciferase reporter plasmids (pCSE). pCSE_del1 (with T1 site deletion from –699 to –691 bp), pCSE_del2 (with T2 site deletion from –47 to –39 bp), and pCSE_del12 (with T1 and T2 site deletions) were synthesized and cloned into pGL3-basic vectors. BxPC3 cells or SW1990 cells were firstly seeded into 24-well plates and cultured to approximately 60% confluence, and then the promoter plasmids and pRL-SV40 vectors were cotransfected into cells for 24 h as previously described [25]. Cells were harvested, and a dual luciferase reporter assay was performed using the Dual-Luciferase Reporter Assay kit (E1910; Promega, Madison, USA) according to the manufacturer's instructions. The firefly luciferase activity normalized to Renilla luciferase activity was considered the promoter activity.

Chromatin immunoprecipitation (ChIP) assay

The chromatin immunoprecipitation (ChIP) assay was performed using the ChIP assay kit (Millipore, Billerica, USA) according to the manufacturer's instructions. Pancreatic cancer cells were seeded into 10-cm dishes and cultured to 60%–70% confluency. After treatment, formaldehyde was added to the cells and incubated at 37°C for 10 min. Then, the cells were scraped off and suspended in1 mL prechilled PBS. Glycine was used to neutralize unreacted formaldehyde. Cell suspensions were lysed in mild RIPA lysis buffer (Beyotime, Shanghai, China) on ice for 30 min and then sonicated to produce chromatin fragments with an average length of 200–1000 bp. The sonicated product was diluted with immunoprecipitation buffer and then incubated with Protein G Agarose for 1 h at 4°C to reduce nonspecific binding. Precleared chromatin solution was incubated with anti-Nrf2 antibody at 4°C overnight, and IgG was used as a negative control. Then, the solution was incubated with Protein G Agarose (MedChemExpress, Shanghai, China) at 4°C for 3 h and centrifuged. The immunoprecipitated DNA was eluted with RIPA elution buffer, purified using spin columns and analyzed by semiquantitative PCR. The 195 bp DNA fragment in the *CSE* promoter region (–148/ + 47 bp) including the Nrf 2 T2 binding site was amplified with the forward primer 5′-GTGACGTTTCAGGCAACGCCT-3′ and the reverse primer 5′-GAGCTAAAGCACGCAGGTAGA-3′.

Statistical analysis

The statistical results are presented as the mean ± SD at least in triplicate. The differences in cell viability, ECAR value, ROS levels and apoptosis were assessed with two-tailed Student's *t*-test between two groups and with one-way analysis of variance (ANOVA) among more than two groups. Differences were considered statistically significant at $P < 0.05$.

Results

KRAS G12D mutation promoted glycolysis and proliferation of pancreatic cancer cells with low ROS levels

KRAS mutations mostly occur in the initiation and development of pancreatic cancer and play important roles during these processes [3–6]. BxPC3 cells express WT KRAS according to the Catalogue Of Somatic Mutations In Cancer (COSMIC) database (https://cancer.sanger.ac.uk/cosmic). We extracted genomic DNA from BxPC3 cells and verified KRAS WT with guanine (G) at the 35th base (Figure 1A). We next employed BxPC3 cells to establish cells overexpressing KRAS WT and G12D mutation which were verified by western blot analysis (Figure 1B). The ECAR value indirectly represents the cellular glycolytic capacity. We found that the ECAR value was significantly upregulated in KRAS mutant BxPC3 cells compared with that in KRAS WT cells (Figure 1C). We next detected cell viability byCCK8 assay *in vitro*. KRAS mutant BxPC3 cells showed higher cell viability than KRAS WT cells (Figure 1D). The rapid proliferation of tumors in a hypoxic environment is accompanied by enhanced aerobic glycolysis, which could cause an increase in intracellular ROS levels [27–29]. However, the intracellular ROS levels were unchanged in KRAS mutant and wild-type typical BxPC3 cells (Figure 1E). These data indicated that KRAS G12D mutationregulated intracellular ROS levels in an unclear manner.

CSE knockdown increased ROS levels and promoted pancreatic cancer cell apoptosis

CSE and cystathionine-β-synthase (CBS) prominently regulate trans-sulfuration metabolism with H_2S production [20,21]. As the third gasotransmitter, H_2S plays important roles in multiple physiological and pathological processes [20,22,23]. H_2S can regulate redox equilibrium in addition to activating signaling pathways [21,22]. Whether CSE or CBS regulates the ROS levels in KRAS mutant cells remains unclear. CSE but not CBS mRNA level was higher in KRAS mutant BxPC3 cells than in KRAS WT cells (Figure 2A). Moreover, western blot analysis results also showed higher CSE protein level, not CBS level, in KRAS mutant BxPC3 cells than in KRAS WT BxPC3 cells (Figure 2B). These results indicated the possible role of CSE in regulating intracellular ROS levels in KRAS-mutant pancreatic cancer. The guanine (G) at the 35th base replaced by adenine (A) was identified in SW1990 cells with G12D mutant KRAS from COSMIC (Supplementary Figure S1A). Therefore, we employed siRNA to knock down *CSE* in BxPC3 cells and SW1990 cells. Western blot analysis results showed that *CSE* knockdown was more significant by si-CSE1 and si-CSE2 in KRAS mutant BxPC3 cells than in KRAS WT BxPC3 cells, the si-CSE1 showed higher knockdown efficiency than si-CSE2 (Figure 2C and Supplementary Figure S1B). We next analyzed cell glycolysis viability by ECAR assay. The ECAR value was significantly decreased after *CSE* knockdown in KRAS mutant BxPC3 cells and SW1990 cells but not in KRAS WT BxPC3 cells (Figure 2D and Supplementary S1C). Moreover, cell viability was also significantly decreased by *CSE* knockdown in KRAS mutant BxPC3 cells and SW1990 cells but not in KRAS WT BxPC3 cells (Figure 2E and Supplementary S1D). The colony formation assay also showed decreased proliferation after *CSE* knockdown in SW1990 cells (Supplementary Figure S1E). The nude mouse xenograft tumor was established through subcutaneous injection of *CSE*-knockdown SW1990 cells by shRNA. The growth of xenograft tumors was decreased when *CSE* was knocked down *in vivo* (Supplementary Figure S1F). Conversely, intracellular ROS levels were increased after *CSE* knockdown in KRAS mutant BxPC3 cells and SW1990 cells, but not in KRAS WT BxPC3 cells (Figure 2F and Supplementary Figure S1G). Meanwhile, cell apoptosis was also increased after *CSE* was knocked down in KRAS mutant BxPC3 cells and SW1990 cells, but not in KRAS WT BxPC3 cells (Figure 2G and Supplementary Figure S1H). These results suggested that *CSE* knockdown increased intracellular ROS levels, promoted cell apoptosis, and

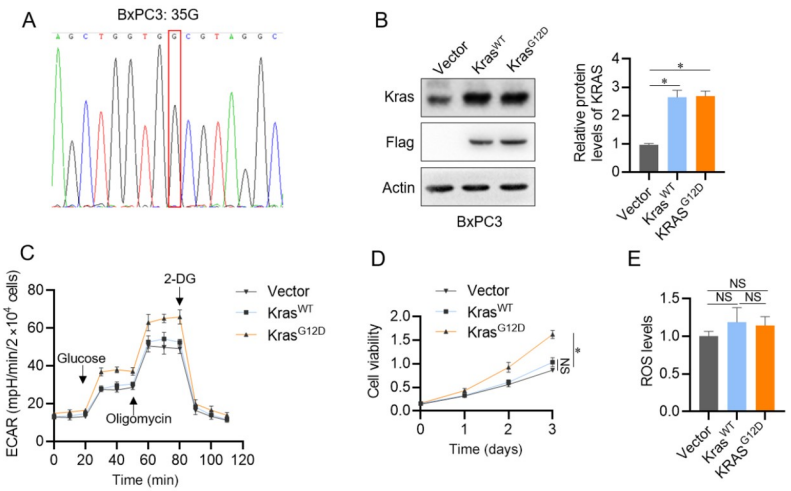

Figure 1. KRAS G12D mutation promoted cell glycolysis and proliferation with low intracellular ROS levels (A) KRAS was identified through DNA sequence in BxPC3 cells. (B) Western blot analysis of BxPC3 cells expressing WT and mutant KRAS. (C–E) The ECAR assay through seahorse, cell proliferation analysis through CCK-8, and intracellular ROS levels detection through flow cytometry were performed in BxPC3 cells *in vitro*. Data are expressed as the mean ± SD, $n = 3$. $^*P < 0.05$.

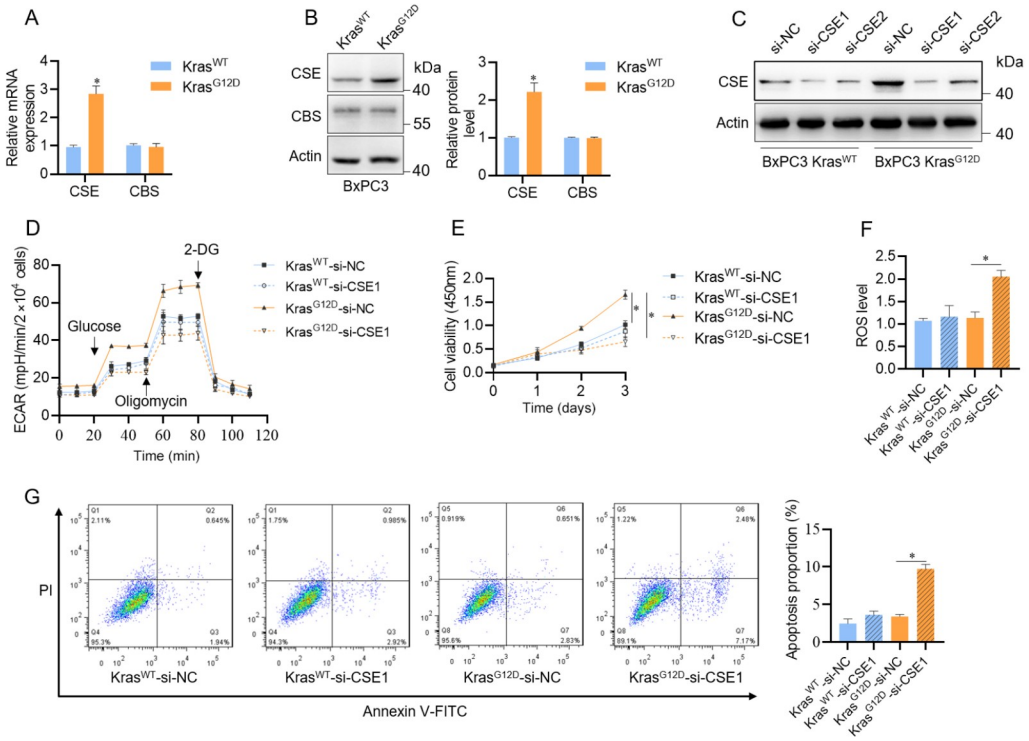

Figure 2. CSE knockdown reduced cell glycolysis and proliferation but upregulated ROS levels and apoptosis in BxPC3 cells (A) CSE and CBS mRNA and (B) protein expression levels were detected by real-time PCR and western blot assay in BxPC3 cells. (C) Western blot analysis of CSE after knockdown by siRNA in BxPC3 cells, the nontargeting siRNAs (si-NC) were used as the control. (D–G) The ECAR assay through seahorse, cell proliferation analysis through CCK-8, intracellular ROS levels detection through flow cytometry, and cell apoptosis measurement through flow cytometry were performed after *CSE* knockdown in BxPC3 cells.

inhibited glycolysis and proliferation in KRAS mutant pancreatic cancer cells.

KRAS mutation activated Nrf2 to promote CSE transcription

Thus, CSE could regulate intracellular ROS levels. Next, we explored the regulatory mechanism of CSE overexpression in KRAS mutant pancreatic cancer cells. The transcription factor Nrf2 is regarded as a master regulator of the cellular antioxidant response through numerous antioxidant and detoxification enzymes for cytoprotection [30–32]. In response to extracellular or intracellular stimuli, Nrf2 is stabilized and translocates to the nucleus to activate the transcription of target genes [32]. KRAS G12D mutation significantly activated the MAPK/ERK pathway, which promoted the upregulation and nuclear localization of Nrf2 (Figure 3A,B). Is the upregulation of CSE expression mediated by Nrf2? We next analyzed CSE mRNA expression in BxPC3 cells after brusatol treatment, an Nrf2 inhibitor (Nrf2-i) which inhibits NRF2 by enhancing protein ubiquitination [33]. Western blot analysis showed that brusatol decreased Nrf2 protein levels in a dose- and time-dependent manner (Supplementary Figure S2C,D). Real-time PCR results showed that CSE mRNA expression was significantly decreased after brusatol treatment in a dose- and time-dependent manner in KRAS mutant BxPC3 cells and SW1990 cells (Figure 3C,D and Supplementary Figure S2A,B). Western blot analysis results also showed a decrease in CSE protein level after brusatol treatment in a dose- and time-dependent manner in KRAS mutant BxPC3 cells and SW1990 cells (Figure 3E,F and Supplementary Figure S2C,D).

We also employed siRNAs to knock down *Nrf2* in BxPC3 stable cells, which was verified by western blot analysis (Figure 3H). CSE mRNA and protein levels were obviously decreased after *Nrf2* knockdown in KRAS mutant BxPC3 cells and SW1990 cells (Figure 3G,H). These results indicated that Nrf2 promoted CSE transcription in KRAS mutant pancreatic cancer cells.

Nrf2 bound to the *CSE* promoter

Next, we explored the regulation of CSE transcription by Nrf2. The sequence of the Nrf2 binding element was identified from the JASPAR database (Figure 4A). The analysis of the *CSE* promoter sequence indicated two possible Nrf2 binding sites (Figure 4B). We cloned the *CSE* promoter sequence (–900 bp to + 50 bp) into the pGL3-Basic plasmid to construct the luciferase reporter plasmid containing the full-length *CSE* promoter (pCSE). Transfection of pCSE plasmids showed obviously increased luciferase activity in KRAS mutant BxPC3 stable cells (Figure 4C). Two potential Nrf2 binding sites were deleted to construct the pCSE_del1 (T1 site deletion), pCSE_del2 (T2 site deletion) and pCSE_del12 (T1 and T2 site deletion) plasmids (Figure 4B). We cotransfected the promoter plasmids pCSE, pCSE_del1, pCSE_del2 and pCSE_del12 with pRL-SV40 into BxPC3 stable cells and SW1990 cells with brusatol treatment or *Nrf2* knockdown. The luciferase activity of pCSE_del1 was not significantly changed, but that of pCSE_del2 and pCSE_del12 showed an obvious decrease compared with the pCSE promoter, and brusatol treatment or *Nrf2* knockdown significantly decreased luciferase activity in KRAS mutant BxPC3 stable cells and SW1990 cells (Figure 4D,E and Supplementary Figure S3A). These

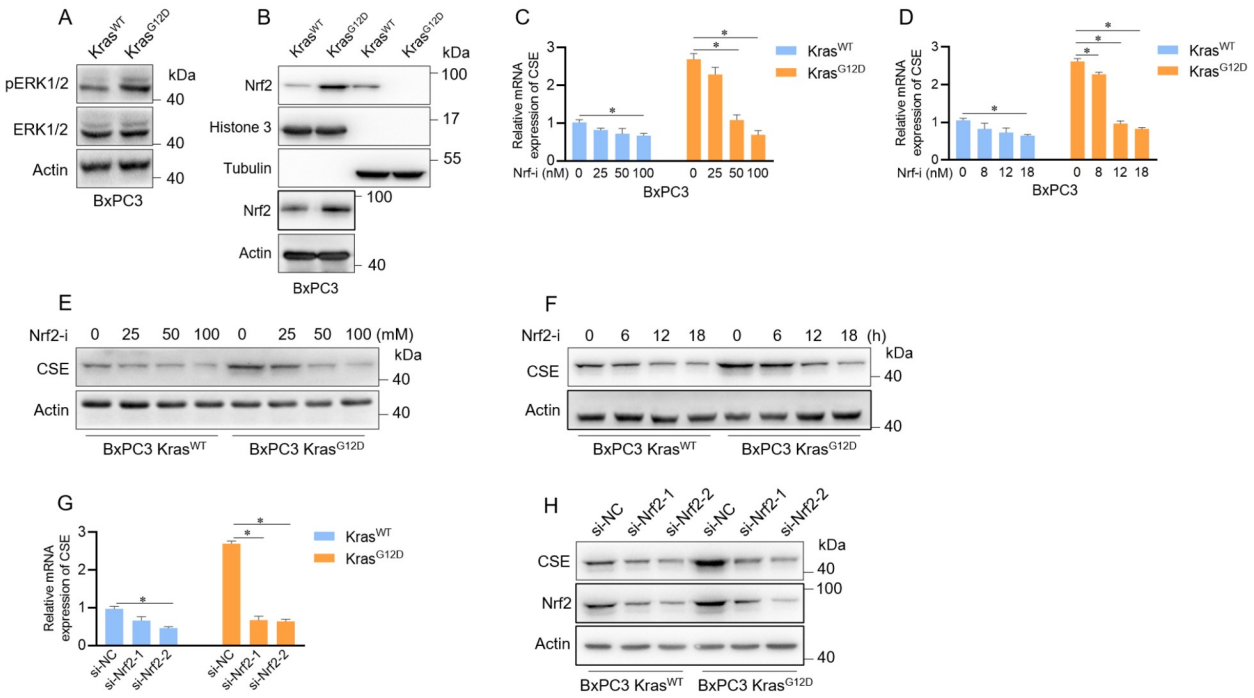

Figure 3. KRAS mutation activated Nrf2 to promote CSE expression in BxPC3 cells (A) The ERK1/2 phosphorylation level was detected through western blot analysis in KRAS WT and G12D mutant BxPC3 cells. (B) The Nrf2 protein level was detected through western blot analysis in whole cell lysate, nuclear and cytoplasm in KRAS WT and G12D mutant BxPC3 cells. (C,D) CSE mRNA expression was detected through real-time PCR in BxPC3 cells after brusatol treatment at the indicated time and concentration. (E,F) CSE protein expression was detected through western blot analysis in BxPC3 cells after brusatol treatment at the indicated time and concentration. (G) CSE mRNA and (H) protein expression levels were detected after *Nrf2* knockdown by siRNAs in BxPC3 cells. Data are presented as the mean ± SD from three independent experiments. $*P < 0.05$.

results indicated that Nrf2 possibly bind with the T2 site of the *CSE* promoter. To further confirm the binding site of Nrf2, we performed a ChIP assay. The 195 bp DNA fragment (–148/ + 47 bp) including the T2 binding site, showed significant amplification in KRAS mutant BxPC3 stable cells and SW1990 cells (Figure 4F and Supplementary Figure S3B). After brusatol treatment, the DNA amplification fragment was inhibited (Figure 4G and Supplementary Figure S3C). When siRNAs were used to knock down Nrf2, the DNA amplification fragment was also decreased (Figure 4H). These results suggested that Nrf2 binding at the T2 site promoted *CSE* transcription.

CSE overexpression and NaHS treatment could recover cell proliferation with ROS elimination

To determine whether KRAS mutation regulates intracellular ROS levels through rhe Nrf2/CSE/H_2Spathway, we established CSE overexpression plasmids with HA tags and then packaged lentivirus to transfect BxPC3 stable cells. The expression of exogenous CSE was verified by western blot analysis (Figure 5A). Next, BxPC3 stable cells were treated with brusatol and transfected with CSE lentivirus. The decreased cell viability after brusatol treatment was recovered by CSE overexpression (Figure 5B), and the increased ROS levels were also eliminated by CSE overexpression in KRAS mutant BxPC3 stable cells (Figure 5C). Next, BxPC3 stable cells were transfected with CSE lentivirus after *Nrf2* knockdown, as shown by western blot analysis (Figure 5D). The decreased viability of KRAS mutant BxPC3 stable cells after *Nrf2* knockdown was recovered by CSE overexpression (Figure 5E), while the increased ROS levels were also quenched (Figure 5F). The H_2S product of CSE plays extensive roles in tumor initiation and development [21,23,24,34,35]. To determine whether H_2S participates in ROS elimination by CSE in KRAS mutant BxPC3 stable cells, NaHS was employed. NaHS treatment recovered the viability of KRAS mutant BxPC3 stable cells after brusatol treatment or *Nrf2* knockdown (Figure 5G,H), and the decreased cell viability by *CSE* knockdown was also rescued by NaHS treatment (Figure 5I). NaHS treatment also eliminated the increased ROS levels induced by brusatol treatment, *Nrf2* knockdown or *CSE* knockdown in KRAS mutant BxPC3 cells (Figure 5J–L). These results suggested that Nrf2 could decrease intracellular ROS levels and promote cell proliferation through CSE/H_2S in KRAS mutant pancreatic cancer cells.

Discussion

KRAS mutations occur in a quarter of human cancers and activate the MAPK pathway in human cancers [36]. KRAS mutations account for 96% of pancreatic ductal adenocarcinoma, playing important roles in PDAC initiation and development [12,36]. Although therapies targeting KRAS are available for lung and colorectal cancer, little effect has been confirmed in PDAC with the increasing number of deaths [12]. Therefore, the exploration of the roles and underlying mechanisms of KRAS mutations is urgent for PDAC therapies. We confirmed that the KRAS G12D mutation promoted tumor cell glycolysis and proliferation in pancreatic cancer. However, rapid growth is often adversely accompanied by excess intracellular ROS production [17–19]. Tumors adopt a series of methods for the antioxidant defense systems [17,19,37]. We found that KRAS mutant pancreatic cancer cells kept rapid proliferation but had low ROS levels. How are intracellular ROS

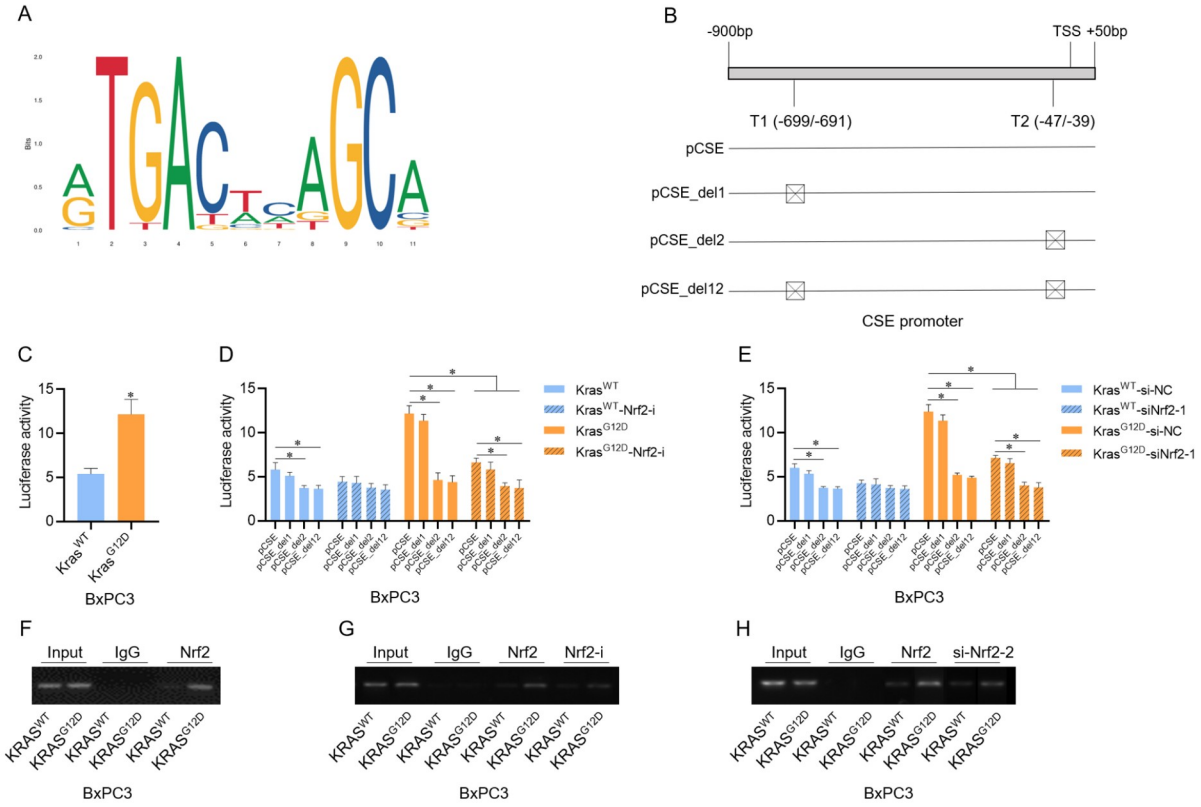

Figure 4. Nrf2 binds tothe T2 site of the *CSE* promoter (A) The binding sequence of Nrf2 from JASPAR. (B) Two potential Nrf2 binding sites were identified in the *CSE* promoter. (C) The luciferase activity of full-length CSE promoter plasmids (pCSE) was detected in BxPC3 cells. (D,E) The luciferase activity of a series of promoter plasmids of pCSE, pCSE_del1 with T1 site deletion, pCSE_del2 with T2 site deletion and pCSE_del12 with T1 and T2 site deletion was detected in BxPC3 cells after Nrf2 inhibition or *Nrf2* knockdown. (F) The DNA fragment of the *CSE* promoter (from –148 to + 47 bp) including the T2 binding site was pulled down and amplified through PCR for detection in BxPC3 cells. (G,H) The DNA fragment of the *CSE* promoter, including the T2 binding site, was detected through ChIP assay in BxPC3 cells after Nrf2 inhibition or *Nrf2* knockdown. Each experiment was independently repeated three times. $*P < 0.05$.

levels regulated in KRAS-mutant PDAC? We focused on key genes involved in the antioxidant regulation.

CSE and CBS, which produce H_2S in the trans-sulfuration pathway, play key roles in regulating the cellular redox equilibrium [22]. Several studies have also reported the roles of CSE/H_2S in promoting tumors [21,24,25,38,39]. We found that KRAS mutation significantly upregulated CSE mRNA and protein levels but not CBS levels. *CSE* knockdown caused a decrease in cell glycolysis and proliferation in KRAS mutant BxPC3 cells. These findings imply the important antioxidant role of CSE in KRAS mutant pancreatic cancer. Therefore, we next explored the regulatory mechanism of CSE expression.

Nrf2 can regulate cellular ROS levels for cytoprotection through target genes [30–32]. However, the Nrf2 protein is rapidly degraded by the ubiquitin–proteasome system in the cytoplasm after translation, in which Kelch-like ECH-associated protein 1 (KEAP1) is an important member of the Cullin 3 (CUL3)-based E3 ubiquitin ligase complex and regulates Nrf2 protein stability and accumulation, and inactivation of KEAP1 is often identified in various tumors [30–32]. KRAS G12D mutation promotes the MAPK/ERK pathway to activate Nrf2. Would CSE transcription be regulated by Nrf2 in KRAS mutant cells? Nrf2 inhibition or *Nrf2* knockdown significantly decreased CSE expression at both mRNA and protein levels, which suggested that Nrf2 regulates CSE expression at the transcription level. Two potential binding sites of Nrf2 in the CSE promoter were identified. We confirmed that the T2 site (–47/–39 bp) plays a key role in regulating CSE transcription. KRAS mutation promotes CSE transcription through Nrf2.

To confirm the roles of the Nrf2/CSE/H_2S axis in the antioxidation in KRAS mutant pancreatic cancer, we transiently transfected CSE-HA plasmids into BxPC3 cells. The decreased cell proliferation viability induced by Nrf2 inhibition or *Nrf2* knockdown could be recovered by CSE overexpression, and the excessive ROS were also eliminated by CSE overexpression. Moreover, the direct addition of NaHS also rescued cell proliferation viability and eliminated excessive ROS. KRAS mutation upregulated CSE transcription through Nrf2 with H_2S production, which promoted cell proliferation and decreased intracellular ROS levels. Altogether, our study revealed that KRAS mutation eliminates intracellular ROS levels and promotes cell proliferation through Nrf2/CSE/H_2S in pancreatic cancer, which provides a potential target for therapy.

Supplementary Data

Supplementary data is available at *Acta Biochimica et Biophysica Sinica* online.

Funding

This work was supported by the grants from the National Natural

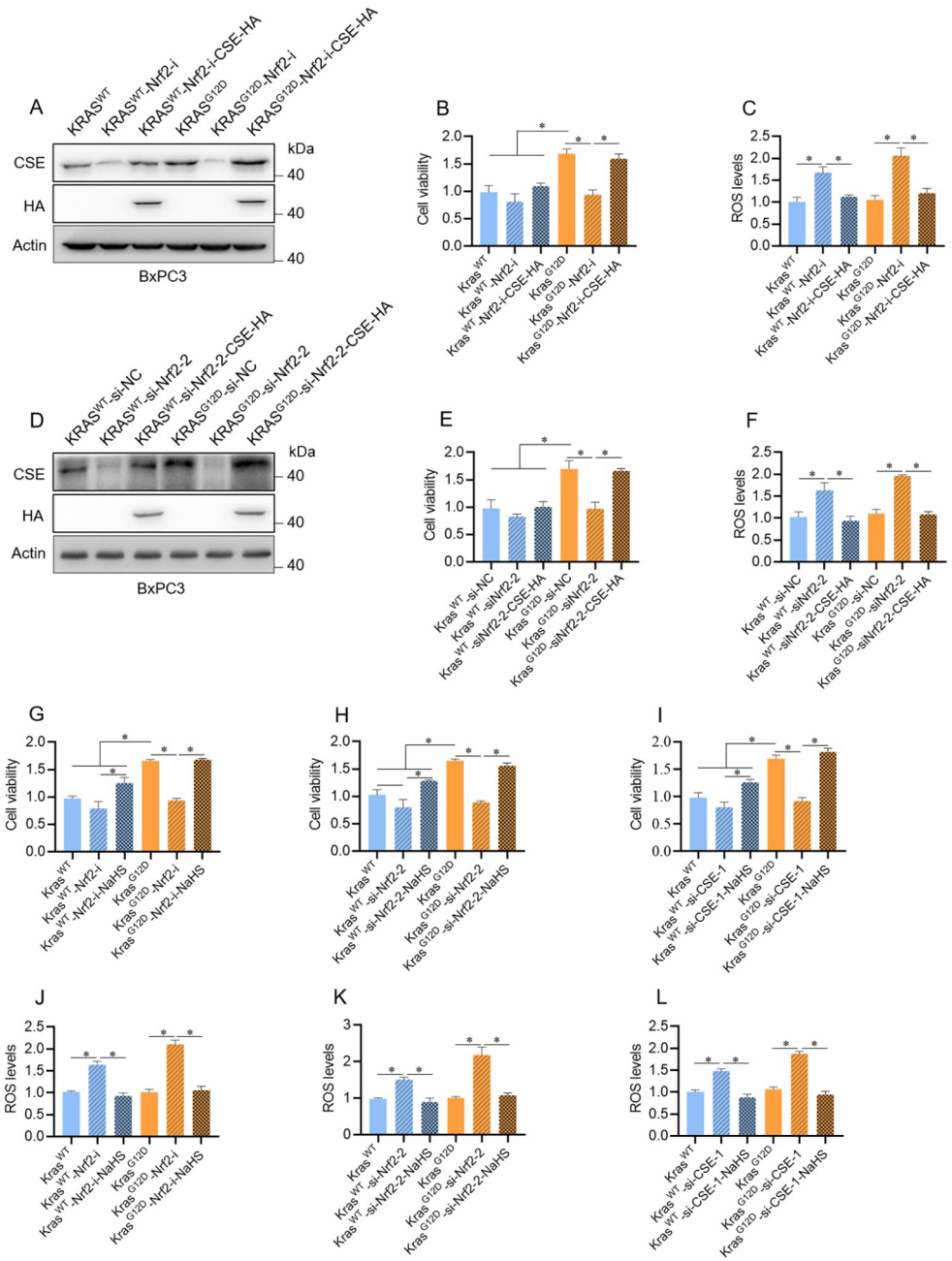

Figure 5. CSE overexpression and NaHS treatment decreased ROS levels to recover cell proliferation (A) Western blot analysis of transiently transfected CSE in BxPC3 cells after Nrf2 inhibition. (B) Cell viability and (C) ROS levels were detected in BxPC3 stable cells after Nrf2 inhibition and transient CSE overexpression. (D) Western blot analysis of transiently transfected CSE in BxPC3 cells after *Nrf2* knockdown. (E) Cell viability and (F) ROS levels were detected in BxPC3 cells after Nrf2 inhibition and transient CSE overexpression. (G–I) Cell viability was detected in BxPC3 cells after Nrf2 inhibition and NaHS treatment, *Nrf2* knockdown and NaHS treatment, *CSE* knockdown and NaHS treatment. (J–L) ROS levels were detected in BxPC3 cells after Nrf2 inhibition and NaHS treatment, *Nrf2* knockdown and NaHS treatment, *CSE* knockdown and NaHS treatment. Data are presented as the mean ± SD from three independent experiments. $^*P < 0.05$.

Science Foundation of China (Nos. 81802751 and 82072682), the JianFeng Project of XuHui Provincial Commission of Health and Family Planning (No. SHXH201703), and the Shanghai Municipal Natural Science Foundation (No. 16411952000).

Conflict of Interest

The authors declare that they have no conflict of interest.

References

1. Fan K, Yang C, Fan Z, Huang Q, Zhang Y, Cheng H, Jin K, *et al.* MUC16 C terminal-induced secretion of tumor-derived IL-6 contributes to tumor-associated Treg enrichment in pancreatic cancer. *Cancer Lett* 2018, 418: 167–175
2. Siegel RL, Miller KD, Jemal A. Cancer statistics, 2020. *CA Cancer J Clin* 2020, 70: 7–30

3. Waddell N, Pajic M, Patch AM, Chang DK, Kassahn KS, Bailey P, Johns AL, *et al.* Whole genomes redefine the mutational landscape of pancreatic cancer. *Nature* 2015, 518: 495–501
4. Cheng H, Fan K, Luo G, Fan Z, Yang C, Huang Q, Jin K, *et al.* KrasG12D mutation contributes to regulatory T cell conversion through activation of the MEK/ERK pathway in pancreatic cancer. *Cancer Lett* 2019, 446: 103–111
5. Wang MT, Holderfield M, Galeas J, Delrosario R, To MD, Balmain A, McCormick F. K-Ras promotes tumorigenicity through suppression of non-canonical wnt signaling. *Cell* 2015, 163: 1237–1251
6. Tape CJ, Ling S, Dimitriadi M, McMahon KM, Worboys JD, Leong HS, Norrie IC, *et al.* Oncogenic KRAS regulates tumor cell signaling via stromal reciprocation. *Cell* 2016, 165: 910–920
7. Hobbs GA, Baker NM, Miermont AM, Thurman RD, Pierobon M, Tran TH, Anderson AO, *et al.* Atypical KRASG12R mutant is impaired in PI3K signaling and macropinocytosis in pancreatic cancer. *Cancer Discovery* 2020, 10: 104–123
8. Ferrer I, Zugazagoitia J, Herbertz S, John W, Paz-Ares L, Schmid-Bindert G. KRAS-mutant non-small cell lung cancer: from biology to therapy. *Lung Cancer* 2018, 124: 53–64
9. Cicenas J, Kvederaviciute K, Meskinyte I, Meskinyte-Kausiliene E, Skeberdyte A, Cicenas J. KRAS, TP53, CDKN2A, SMAD4, BRCA1, and BRCA2 mutations in pancreatic cancer. *Cancers* 2017, 9: 42
10. Ryan MB, Fece DLCF, Phat S, Myers DT, Wong E, Shahzade HA, Hong CB, *et al.* Vertical pathway inhibition overcomes adaptive feedback resistance to KRASG12C inhibition. *Clin Cancer Res* 2020, 26: 1633–1643
11. Bamford S, Dawson E, Forbes S, Clements J, Pettett R, Dogan A, Flanagan A, *et al.* The COSMIC (Catalogue of Somatic Mutations in Cancer) database and website. *Br J Cancer* 2004, 91: 355–358
12. Waters AM, Der CJ. KRAS: the critical driver and therapeutic target for pancreatic cancer. *Cold Spring Harb Perspect Med* 2018, 8: a031435
13. Gopinathan A, Morton JP, Jodrell DI, Sansom OJ. GEMMs as preclinical models for testing pancreatic cancer therapies. *Dis Model Mech* 2015, 8: 1185–1200
14. Aguirre AJ, Bardeesy N, Sinha M, Lopez L, Tuveson DA, Horner J, Redston MS, *et al.* Activated Kras and *Ink4a/Arf* deficiency cooperate to produce metastatic pancreatic ductal adenocarcinoma. *Genes Dev* 2003, 17: 3112–3126
15. Hingorani SR, Wang L, Multani AS, Combs C, Deramaudt TB, Hruban RH, Rustgi AK, *et al.* Trp53R172H and KrasG12D cooperate to promote chromosomal instability and widely metastatic pancreatic ductal adenocarcinoma in mice. *Cancer Cell* 2005, 7: 469–483
16. Hingorani SR, Petricoin Iii EF, Maitra A, Rajapakse V, King C, Jacobetz MA, Ross S, *et al.* Preinvasive and invasive ductal pancreatic cancer and its early detection in the mouse. *Cancer Cell* 2003, 4: 437–450
17. Sosa V, Moliné T, Somoza R, Paciucci R, Kondoh H, LLeonart ME. Oxidative stress and cancer: an overview. *Ageing Res Rev* 2013, 12: 376–390
18. Cadenas S. Mitochondrial uncoupling, ROS generation and cardioprotection. *Biochim Biophys Acta Bioenerg* 2018, 1859: 940–950
19. Prasad S, Gupta SC, Tyagi AK. Reactive oxygen species (ROS) and cancer: role of antioxidative nutraceuticals. *Cancer Lett* 2017, 387: 95–105
20. Chiku T, Padovani D, Zhu W, Singh S, Vitvitsky V, Banerjee R. H2S biogenesis by human cystathionine γ-lyase leads to the novel sulfur metabolites lanthionine and homolanthionine and is responsive to the grade of hyperhomocysteinemia. *J Biol Chem* 2009, 284: 11601–11612
21. Fan K, Li N, Qi J, Yin P, Zhao C, Wang L, Li Z, *et al.* Wnt/β-catenin signaling induces the transcription of cystathionine-γ-lyase, a stimulator of tumor in colon cancer. *Cell Signal* 2014, 26: 2801–2808
22. Kimura Y, Goto YI, Kimura H. Hydrogen sulfide increases glutathione production and suppresses oxidative stress in mitochondria. *Antioxid Redox Signal* 2010, 12: 1–13
23. Hellmich MR, Szabo C. Hydrogen sulfide and cancer. *Handb Exp Pharmacol* 2015, 230: 233–241
24. Cai WJ, Wang MJ, Ju LH, Wang C, Zhu YC. Hydrogen sulfide induces human colon cancer cell proliferation: role of Akt, ERK and p21. *Cell Biol Int* 2010, 34: 565–572
25. Yin P, Zhao C, Li Z, Mei C, Yao W, Liu Y, Li N, *et al.* Sp1 is involved in regulation of cystathionine γ-lyase gene expression and biological function by PI3K/Akt pathway in human hepatocellular carcinoma cell lines. *Cell Signal* 2012, 24: 1229–1240
26. Fan K, Wang J, Sun W, Shen S, Ni X, Gong Z, Zheng B, *et al.* MUC16 C-terminal binding with ALDOC disrupts the ability of ALDOC to sense glucose and promotes gallbladder carcinoma growth. *Exp Cell Res* 2020, 394: 112118
27. Lee N, Kim D. Cancer metabolism: fueling more than just growth. *Molecules Cells* 2016, 39: 847–854
28. Rodic S, Vincent MD. Reactive oxygen species (ROS) are a key determinant of cancer's metabolic phenotype. *Int J Cancer* 2018, 142: 440–448
29. Hanahan D, Weinberg RA. Hallmarks of cancer: the next generation. *Cell* 2011, 144: 646–674
30. Rojo DLVM, Chapman E, Zhang DD. NRF2 and the hallmarks of cancer. *Cancer Cell* 2018, 34: 21–43
31. Bellezza I, Giambanco I, Minelli A, Donato R. Nrf2-Keap1 signaling in oxidative and reductive stress. *Biochim Biophys Acta Mol Cell Res* 2018, 1865: 721–733
32. Tonelli C, Chio IIC, Tuveson DA. Transcriptional regulation by Nrf2. *Antioxid Redox Signal* 2018, 29: 1727–1745
33. Cai SJ, Liu Y, Han S, Yang C. Brusatol, an NRF2 inhibitor for future cancer therapeutic. *Cell Biosci* 2019, 9: 45
34. Youness RA, Gad AZ, Sanber K, Ahn YJ, Lee GJ, Khallaf E, Hafez HM, *et al.* Targeting hydrogen sulphide signaling in breast cancer. *J Adv Res* 2021, 27: 177–190
35. Pan Y, Ye S, Yuan D, Zhang J, Bai Y, Shao C. Hydrogen sulfide (H2S)/cystathionine γ-lyase (CSE) pathway contributes to the proliferation of hepatoma cells. *Mutat Res* 2014, 763-764: 10–18
36. Drosten M, Barbacid M. Targeting the MAPK pathway in KRAS-driven tumors. *Cancer Cell* 2020, 37: 543–550
37. Yuan F, Woollard JR, Jordan KL, Lerman A, Lerman LO, Eirin A. Mitochondrial targeted peptides preserve mitochondrial organization and decrease reversible myocardial changes in early swine metabolic syndrome. *Cardiovasc Res* 2018, 114: 431–442
38. Cao X, Zhang W, Moore PK, Bian J. Protective smell of hydrogen sulfide and polysulfide in cisplatin-induced nephrotoxicity. *Int J Mol Sci* 2019, 20: 313
39. Wang L, Shi H, Liu Y, Zhang W, Duan X, Li M, Shi X, *et al.* Cystathionine-γ-lyase promotes the metastasis of breast cancer via the VEGF signaling pathway. *Int J Oncol* 2019, 55: 473